Assessment of droop and VSM equivalence considering the cascaded control dynamics

Sam Harrison[1], Callum Henderson[1], Panagiotis N. Papadopoulos[1], Agusti Egea-Alvarez[1]*

[1]*University of Strathclyde, Glasgow, United Kingdom*
**sam.harrison@strath.ac.uk*

Keywords: DC-AC POWER CONVERTERS, DROOP CONTROL, VIRTUAL SYNCHRONOUS MACHINE

Abstract

Grid Forming (GFM) converters are changing the way that power converters interact with the network to resemble synchronous machines (SM). Several GFM technologies including the Synchronverter, a particular member of Virtual Synchronous Machine (VSM), and GFM droop, based on standard current control and droop, have been suggested. The controllers have been compared and found to be equivalent to each other in steady state. The equivalence generally focusses on individual operating conditions and fails to address differences in dynamic properties. This paper provides a clear tuning guide of both controls in terms of SM properties and a discussion of the analytical equivalence using the output of time-domain medium-voltage DC (MVDC) converter models. Initially, the GFM droop is found to be less damped despite the equivalent tuning in terms of damping ratio. A parametric sweep of the cascaded control present within the GFM droop finds that the Voltage Control bandwidth and proportional gain can be tuned to adjust the damping of the response. The Voltage Control parameters are also found to affect the GFM droop's stability.

1 Introduction

Power systems are experiencing a reduction in synchronous machines (SMs) due to the increase in converter interfaced devices such as renewable energy sources (RESs) [1]. The reduction in SMs coincides with a reduction in synchronous inertial energy storage, which has historically been a key feature for a system's frequency stability by responding to power imbalances on short timescales. The inertial storage arrests the initial frequency change before a slower governor-droop response adjusts SM capacity to re-balance the system. Low inertia levels are recognised as a key issue facing European System Operators [2] who will otherwise be forced to constrain the fraction of RESs that provide a system's power demand to maintain stability.

Another key issue associated with the rapid uptake of RESs is the overloading of distribution networks [3]. The RESs are often connected at medium voltage levels, altering the previously unidirectional flow of power and forcing the network towards its transfer limits. Voltage deviations resulting from the intermittent RESs and inflexible AC networks can also reduce the reliability of the power supply. Medium-voltage DC (MVDC) links are being proposed to solve these issues [4-5]. Traditional radial networks can be reinforced using the MVDC links, creating meshed hybrid AC-DC networks [4]. The MVDC links are interfaced by highly controllable converters that can achieve bi-directional flow and reactive power compensation and hence higher network utilisation [5]. MVDC is also fount be a cost-effective solution for offshore wind farms [6].

The majority of converter interfaced devices are not electromagnetically linked to the grid so cannot provide inertial power naturally. However, converter control can be adapted to provide a rapid response to contain the AC grid frequency [7]. The conventional converter Current Control (CC) is grid following, as it uses a phase-locked loop (PLL) to synchronise the converter voltage with the grid voltage. CC can be adapted to provide both droop response and an inertial injection [8]. As the CC acts as a current source it is capable of good overcurrent limitation [9], however, it cannot strengthen the grid (beyond the rapid power injections) as a stiff SM voltage source would.

Grid forming (GFM) control has gained interest for future power systems as it enables converters to appear as a stiff voltage source that provides desirable SM functionality including, but not limited to, inertia provision [10]. Virtual synchronous machines (VSMs) are a subgroup of GFMs that implement the swing equation within the control in varying forms and degrees of complexity [11-13]. The virtual inertial constant is set within the swing equation while the droop response is often included implicitly in the form of a virtual damping. GFM droop controls have also been developed that set the converter angle according to a measured power imbalance and are shown to provide an inertial response equivalent to a VSM when a low-pass filter (LPF) is applied to the power measurement [14]. The equivalence between the two GFM controls has been discussed but the dynamic properties of each power response to a frequency disturbance have not been explored across the full range of control tuning.

An initial assessment highlights that the GFM droop possesses the same steady state behaviour as a VSM, but the transient responses are different due to the cascaded Voltage and Current Control present in the droop [14]. The presence of both GFM droop and VSM controls on a power system are found to improve the frequency stability due to the fast synchronisation, however, the resulting frequency excursions are not identical [15], confirming that each control possesses different dynamic properties. The different implementation of the inertia forces

This is a peer reviewed, accepted author manuscript of the following research article: Harrison, S., Henderson, C., Papadopoulos, P. N., & Egea-Alvarez, A. (2021). Assessment of droop and VSM equivalence considering the cascaded control dynamics. In The 17th International Conference on AC and DC Power Transmission (ACDC 2021) (Vol. 2021, pp. 126-131). [9692715] IET. https://doi.org/10.1049/icp.2021.2456

the two control responses to be significantly different when each is subject to a power reference step change [16]. [16] also details an adapted VSM, which emulates the separate channels of a SM that provide damping and droop independently, and highlights that the GFM droop cannot provide the same level of damping. An adapted GFM droop control is formed by adding a lead-unit to act on the power error and is proven to equate to the adapted VSM [17].

This paper aims to assess the accuracy of the analytical comparison of GFM droop to VSM control. The controls will be tuned in terms of SM properties using a conventional equivalent transfer function (tf) method [18,19] and the equivalency will be assessed for a representative MVDC converter. As well as the control's stability, the dynamic properties, which are often neglected, are considered as these features will ultimately affect the ability for each control to support the AC grid frequency [15]. The impact of the cascaded control on the power response (not yet considered throughout the literature) will be assessed by comparing the GFM droop time-domain model's responses as the Current and Voltage Control parameters are varied.

2 Modelling and control equivalence

The equivalence between GFM droop control and VSM control, as discussed in [14,16-18], is assessed by deriving tfs of each control, comparing the second order system properties of these models with equivalent SM properties, and tuning the controls to achieve desired inertia responses and damping ratios. The equivalent tunings are then applied to time-domain MVDC converter models with each control connected to an infinite bus representation of an AC power system, as detailed in [20]. The time-domain model parameters are shown in Table 1, alongside the base control tuning parameters.

Table 1 Time-domain model base scenario parameterisation.

Parameter name	Parameter label	Parameter value
Base AC voltage	$V_n \approx V_0$	1 (kV)
DC voltage	V_{DC}	2.5 (kV)
Base impedance	Z_n	0.1 (Ω)
Filter resistance	R_f	1.6 (mΩ)
Filter inductance	L_f	50.516 (μH)
Rated power	S_n	10 (MW)
Reactive power reference	Q^*	0 (MVAr)
Active power reference	P^*	1 (MW)
Base frequency	ω_0	50 (Hz)
Reactive power droop	$K_{qD} = \frac{1}{D_q}$	$0.1\frac{\omega_0}{S_n}\left(\frac{Hz}{MW}\right)$
Reactive power LPF cut-off frequency	$\omega_q = \frac{1}{\tau_q K_{qD}}$	1 (Hz)
CC bandwidth	ω_{CC}	1000 (Hz)
VC bandwidth	$\omega_{VC} \approx K_{iV}$	100
VC proportional gain	$K_{p,VC}$	40

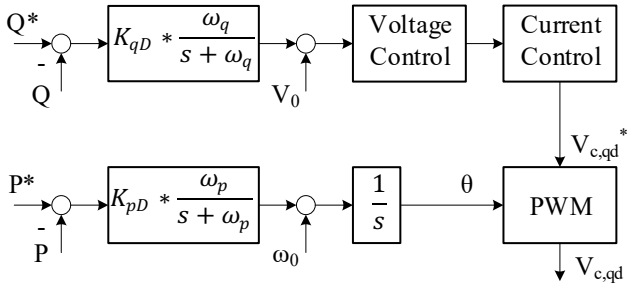

Fig.1 GFM droop control diagram.

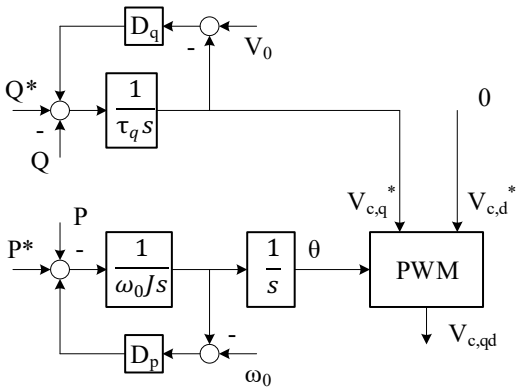

Fig.2 Synchronverter control diagram.

The GFM droop control, pictured in Fig.1, is based on the power control strategy described in [21]. Both the converter angle θ and voltage magnitude references $V^*_{c,qd}$ are determined according to two droop constants, K_{pD} and K_{qD}, that act on the active or reactive power error relative to the references, P^* and Q^* respectively. A second order dynamic (inertial response) appears due to the implementation of the LPF on the active power channel [14]. The frequency and voltage deviations are added to their respective base values, ω_0 and V_0, following the LPF. The GFM droop is implemented with cascaded Voltage and Current Controls that use the voltage magnitude reference to set current references for the waveform modulation. The cascaded control features a simple PI voltage controller and the conventional Current Control, both detailed in [21].

The VSM scheme, pictured in Fig.2, is based on the Synchronverter strategy described in [12]. The Synchronverter uses SM dynamic equations, incorporating virtual inertia J and reactive power time constant τ_q, to set the voltage angle and magnitude references. The Synchronverter's droop and damping responses are forced in a single feedback channel by comparing the virtual rotor frequency with a frequency reference ω_0, multiplying this error by a virtual damping D_p, and adding this power to the power reference. The Synchronverter feeds the voltage references directly to the waveform modulation without any cascaded control.

2.1 Synchronous machine dynamic model

A common approach to assess SM properties during the initial period following a frequency disturbance uses a transfer function (tf) to represent a linearised box model of the machine

in the Laplace domain [19]. This tf is used to tune the controllers to provide equivalent SM properties and to assess the controllability of the strategies. The conventional SM box model only includes the swing equation dynamics as the slow time constant of the prime mover means that the SM droop does not respond on short timescales [19]. However, the time constant of a converter is very short [10], and as both considered controls include a droop component in some form, the SM droop dynamics must also be considered. The resulting tf that describes a SM's electric power output response (P_{out}) to a grid frequency disturbance (ω_g) is:

$$\frac{P_{out}(s)}{\omega_g(s)} = \frac{-K_s s - \frac{K_{\omega D}\omega_0 K_s}{2HS_n}}{s^2 + \frac{(K_{\omega D}+K_d)\omega_0}{2HS_n}s + \frac{K_s\omega_0}{2HS_n}} \quad (1)$$

Where $K_s \approx \frac{V_n^2}{\omega_0(L_f+L_g)}$ is the synchronising torque that is dependent on grid properties (where L_g is the grid inductance) and is assumed to be equal for the SM and converter devices [19]. $K_{\omega D}$ is the $\omega \rightarrow P$ droop constant, ω_0 is the synchronous speed, H is the inertia constant, S_n is the rated power, and K_d is the damping coefficient. The natural frequency (ω_n) and damping ratio (ζ) of the system can be found by comparing the characteristic equation with its standard second order form:

$$\omega_n = \sqrt{\frac{K_s\omega_0}{2HS_n}}; \zeta = \frac{K_{\omega D}+K_d}{2}\sqrt{\frac{\omega_0}{2HS_nK_s}} \quad (2)$$

2.2 Converter control dynamic models and tuning

The GFM droop control is represented by the following tf:

$$\frac{P_{out}(s)}{\omega_g(s)} = \frac{-K_s s - \omega_p K_s}{s^2 + \omega_p s + K_s K_{pD}\omega_p} \quad (3)$$

Where ω_p is the cutoff frequency of the active power LPF and the $P \rightarrow \omega$ droop constant is $K_{pD} = \frac{1}{K_{\omega D}}$. The resulting natural frequency and damping ratio of the droop control are:

$$\omega_n = \sqrt{K_s K_{pD}\omega_p}; \zeta = \frac{1}{2}\sqrt{\frac{\omega_p}{K_s K_{pD}}} \quad (4)$$

According to (4), the GFM droop possesses two control parameters that can be tuned to achieve a given frequency response: ω_p and K_{pD}. However, there exists at least three features that might be desired from a frequency supporting MVDC link: the inertial response, the droop response, and the damping ratio of the response. Therefore, the operator must choose the two desired frequency response properties and tune the converter to achieve these, accepting the final resulting property. Any combination of two frequency response properties can be set for the GFM droop using the relationships between (2) and (4).

The Synchronverter control is represented by the following tf:

$$\frac{P_{out}(s)}{\omega_g(s)} = \frac{-K_s s - \frac{K_s D_p}{\omega_0 J}}{s^2 + \frac{D_p}{\omega_0 J}s + \frac{K_s}{\omega_0 J}} \quad (5)$$

Where D_p is the virtual damping and J is the virtual moment of inertia. The natural frequency and damping ratio of the system are:

$$\omega_n = \sqrt{\frac{K_s}{\omega_0 J}}; \zeta = \frac{D_p}{2\sqrt{\omega_0 J K_s}} \quad (6)$$

Two control parameters are also available for the Synchronverter to tune the frequency response, however, there is only one tuning approach that can describe a Synchronverter in terms of SM properties. The inertia can be set explicitly via $J = \frac{2HS_n}{\omega_0^2}$, confirmed by comparing the natural frequency in (2) with the natural frequency in (6). The Synchronverter must then be defined in terms of damping ratio as the droop response cannot be set explicitly, unlike the GFM droop. The droop cannot be set explicitly as the virtual damping describes a combination of the SM droop and damping coefficients: $D_p = K_{\omega D} + K_d$, proven by comparing the damping ratios of (2) and (6). The Synchronverter droop can then be determined indirectly by calculating the droop response of a GFM droop that has the same inertia constant and damping ratio using (4) and (6). The combined droop and damping action of the simple Synchronverter is identified in [16] who proposes the implementation of a frequency identifier, such as a PLL, to feed a separate channel that enables isolated damping from the droop response. However, the simple Synchronverter without the additional frequency identifier is considered for the purposes of this study to maintain similarity to the GFM droop that also doesn't use a frequency identifier.

3 Methodology

The tuning guide detailed in Section 2 attempts to equate the GFM droop and Synchronverter controls, as reported in [14]. Using this guide, the time-domain converter models are tuned to achieve a range of inertia constants $H = 0.5{:}\,5\ s$ (a representative range for a SM [19]) and damping ratios $\zeta = 0.5{:}\,1.5$. The higher damping scenarios correspond to a higher droop response as $K_{\omega D} + K_d$ are the remaining parameters that can vary with ζ for a SM that has a given H, K_s, S_n, and ω_0, according to (2). The short circuit ratio (SCR) is also varied as a proxy to assess the power system strength. All of the control tunings are tested on very weak $SCR < 2$, weak $SCR = 2$, and strong systems $SCR = 5$ [22]. The SCR is set using the grid resistance $R_g = \frac{0.01 Z_n}{SCR}$ and grid inductance $L_g = \frac{Z_n}{\omega_0 SCR}$.

A frequency disturbance of 1 Hz, with a rate of change of frequency $ROCOF = 0.5\ Hz/s$, is forced on the infinite bus AC power system at t=1 s to analyse each control configuration's power response. The accuracy of the GFM droop and Synchronverter equivalence is assessed by comparing the time-domain model power outputs in terms of steady state stability and dynamic response.

[15-16] suggest that the control equivalence is not always true, so a parametric sweep is carried out to identify if differences in the control properties are introduced by the GFM droop's cascaded control. The bandwidths of both the Current Control

(CC) and the Voltage Control (VC) are assessed by subjecting a range of time-domain control configurations to the frequency disturbance and comparing the power responses. The bandwidth of the Current Control (ω_{CC}) can be set according to:

$$K_{p,CC} = L_f \omega_{CC};\ K_{i,CC} = R_f \omega_{CC} \quad (7)$$

Where $K_{p,CC}$ and $K_{i,CC}$ are the CC proportional and integral gains. The Current Control bandwidth is varied from $\omega_{CC} = 100{:}\,100{:}\,1100\ Hz$. The integral gain of the voltage controller ($K_{i,VC}$) can be used as a proxy for the VC bandwidth (ω_{VC}). The VC integral gain is varied from $K_{i,VC} = 10{:}\,10{:}\,110$. The VC proportional gain is also varied, from $K_{p,VC} = 4{:}\,4{:}\,52$, to assess if this control parameter affects the control response.

4 Results and analysis

The time-domain control models are tuned in terms of a range of SM properties and are subject to the frequency disturbance. The results are presented in three parts. Section 4.1 compares the steady state and dynamic features of the time-domain responses to the frequency disturbance by the GFM droop (with base cascaded control configuration) and the Synchronverter. Section 4.2 assesses if any of the properties of the GFM droop response depend on the CC bandwidth. Section 4.3 identifies if either the VC bandwidth (integral gain) or proportional gain impact the dynamics or stability of the GFM droop response.

4.1 Dynamic response equivalence

Fig.3 compares the equivalently tuned controls for two scenarios. As discussed in the literature [14,16-18] and in Section 2, the analytical equivalence enables the GFM droop and Synchronverter controls to be tuned to provide equivalent steady-state behaviour. When both controls are stable, as in Fig.3, the steady-state equivalence is exhibited by the equal droop response for the given frequency disturbance, a by-product of the chosen H, ζ, and SCR.

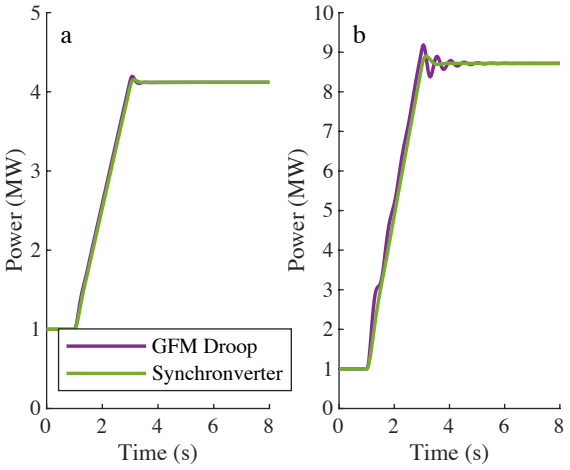

Fig.3 Comparison of GFM droop and Synchronverter dynamic response to frequency disturbance for base tuning detailed in Table 1 for control configuration (a) $H = 0.5\ (s)$ and $\zeta = 0.7$ on grid with $SCR = 1.7$ and (b) $H = 2\ (s)$ and $\zeta = 0.6$ on grid with $SCR = 5$.

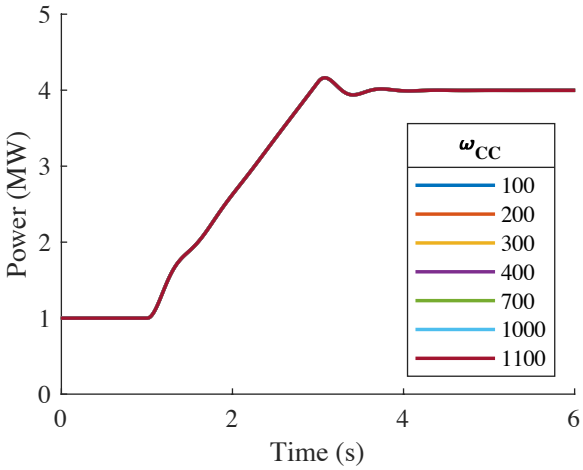

Fig.4 Comparison of GFM droop dynamic response to frequency disturbance for control configuration $H = 1\ (s)$, $\zeta = 0.5$, and $K_{i,VC} = 100$ on grid with $SCR = 1.5$ as the CC bandwidth (ω_{CC}) is varied.

The controls are not equivalent in terms of dynamic response. Fig.3(a) shows the response of both controls when tuned to achieve an equivalent damping ($\zeta = 0.7$) for the $\omega_g \rightarrow P_{out}$ tfs (3-6). Despite the equivalent tuning, the GFM droop control appears to be less damped than the Synchronverter. The reduced damping in GFM droop compared to an equivalent Synchronverter is more apparent in the higher inertia case in Fig.3(b). Similar differences between the dynamic response of GFM droop with cascaded control and open loop PWM VSM are identified in [14]. As the simple Synchronverter strategy assessed here does not implement any additional damping branches that can drive differences in dynamic response [16-17], and the $\omega_g \rightarrow P_{out}$ tf does not consider the impact of the cascaded control, the difference must either stem from the cascaded control or due to a non-equivalence between the two GFM strategies.

4.2 Impact of cascaded Current Control

The results of the CC parametric sweep are shown in Fig.4 for a stable, low SCR, GFM droop configuration with the base VC bandwidth ($K_{i,VC}$). Selected steps of the CC sweep are pictured but the large range of bandwidths does not appear to impact the stability or the dynamics of the power response of the time-domain model. The CC bandwidth remains significantly higher that the GFM dynamics suggesting that the assumption of unity action by the CC in the literature [18] remains accurate when assessing the response to frequency disturbances.

4.3 Impact of cascaded Voltage Control

A GFM droop configuration (that the Synchronverter is stable for) with the base CC bandwidth is shown in Fig.5 throughout stages of the VC bandwidth sweep. The VC integral gain (the proxy for VC bandwidth) is shown to impact the dynamic response. Lowering the VC bandwidth decreases the response speed, forcing the GFM droop to appear more like the inherently damped Synchronverter. The bandwidth can be reduced to the lowest tested value $K_{i,VC} = 10$ without the response becoming unstable. However, Fig. 6 exhibits the

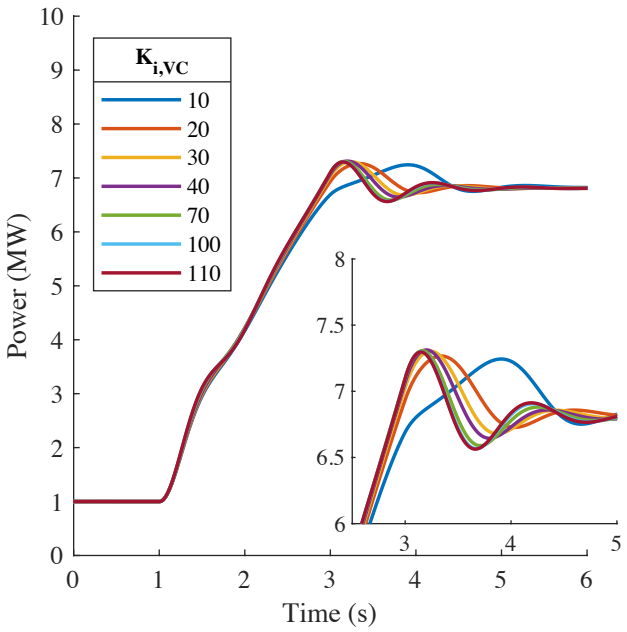

Fig.5 Comparison of GFM droop dynamic response to frequency disturbance for control configuration $H = 3\ (s)$, $\zeta = 0.5$, and ω_{CC}=1000 on grid with $SCR = 2$ as the VC bandwidth ($K_{i,VC}$) is varied.

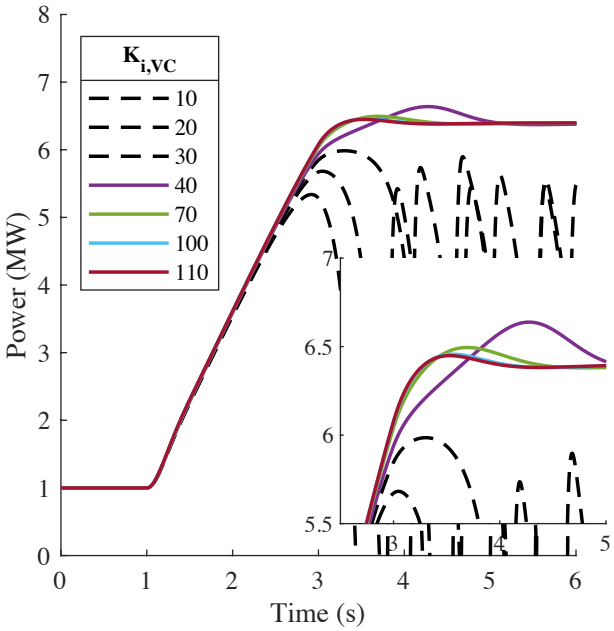

Fig.6 Comparison of GFM droop dynamic response to frequency disturbance for control configuration $H = 1\ (s)$, $\zeta = 0.9$, and ω_{CC}=1000 on grid with $SCR = 1.5$ as the VC bandwidth ($K_{i,VC}$) is varied. Dashed lines indicate control configurations that are destabilised following the disturbance.

GFM droop behaviour throughout the VC bandwidth sweep for a configuration that the Synchronverter is not stable for. Again, the dynamic response is slowed as the bandwidth is reduced until $K_{i,VC} = 30$ where the GFM droop is driven to instability following the frequency disturbance, like the Synchronverter. Decreasing the VC bandwidth is also capable of stabilising certain GFM droop configurations that are unstable for the base tuning. For example, base tuning configurations that are insufficiently damped are stabilised by

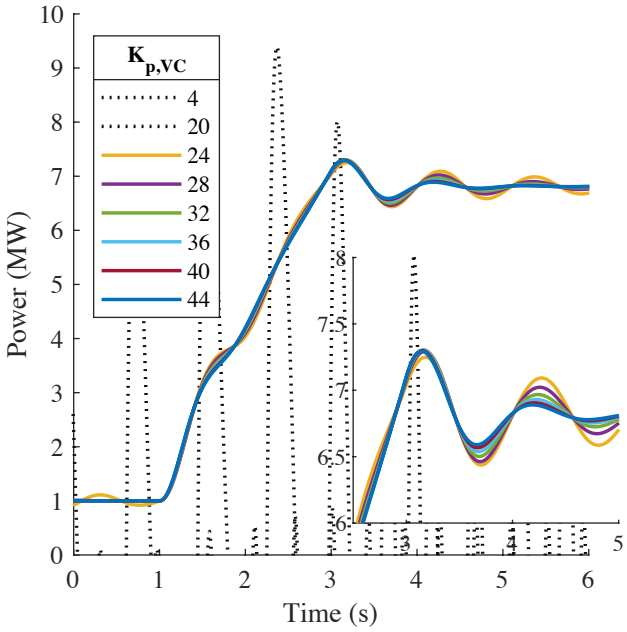

Fig.7 Comparison of GFM droop dynamic response to frequency disturbance for control configuration $H = 3\ (s)$, $\zeta = 0.5$, ω_{CC}=1000, and $K_{i,VC} = 100$ on grid with $SCR = 2$ as the VC proportional gain ($K_{p,VC}$) is varied. Dashed lines indicate control configurations that are destabilised before the disturbance.

a lower VC bandwidth (e.g. $H = 5\ s, \zeta = 0.5, SCR = 5$).

Extreme low (but stable) GFM droop VC bandwidths exhibit a delayed power peak almost 1 second after the end of the frequency disturbance (Fig.5 and Fig.6). The $K_{i,VC} = 40$ peak for the lower SCR scenario in Fig.6 exceeds any peaks experienced by the higher bandwidths, whereas the final tested $K_{i,VC} = 10$ peak in Fig.5 remains lower than other peaks. This suggests that boundary VC bandwidths preceding the GFM droop's stability limits may not improve the equivalence to the Synchronverter response. Low VC integral gains away from stability boundaries ($K_{i,VC} \approx 50$) should be used to achieve a GFM droop response more equivalent to the Synchronverter.

Fig.7 pictures the GFM droop response to the frequency disturbance for the base CC and VC bandwidths as the VC proportional gain is varied. The VC proportional gain is also found to affect both the GFM droop stability and dynamic properties. The response is driven to instability for low proportional gains $K_{p,VC} \leq 20$. However, unlike the VC bandwidth, these low values are unable to converge to a stable operating point from the simulation initiation and are not destabilised by the disturbance. The dynamic response is also affected; larger proportional gains correspond to a higher response damping. Therefore, a high proportional gain should be used to increase the equivalence between the GFM droop and Synchronverter responses. The response dynamics experience similar changes when $K_{p,VC}$ is varied for lower VC bandwidths (e.g. $K_{i,VC} = 50$) but the limits of stable operation change (not pictured).

5 Conclusion

This paper provides a clear tuning guide and discussion of the equivalence between GFM droop and Synchronverter controls, with consideration of the GFM droop's cascaded controls. The study highlights the apparently lower damping of the GFM droop despite the equivalent tuning. The comparison also shows that the steady-state equivalence does not hold for all values of inertia, damping, and short circuit ratio. A parametric sweep shows that the GFM droop's cascaded Voltage Control bandwidth and proportional gain can be adapted to adjust the response damping. The Voltage Control parameters are also found to affect the controller's stability. A low VC bandwidth and high proportional gain are suggested to enable the GFM droop to better resemble the Synchronverter. However, tuning these control parameters does not allow a complete emulation of the Synchronverter dynamic response and stable operating region. Therefore, there remains some inequality between the two controls.

6 Acknowledgements

This work was supported by the Engineering and Physical Sciences Research Council, Grant Reference: EP/L016680/1, and by the UKRI Future Leaders Fellowship MR/SO34420/1.

7 References

[1] Ofgem, "Electricity generation mix by quarter and fuel source (GB) April 2021," Apr. 2021. 2021 https://www.ofgem.gov.uk/data-portal/electricity-generation-mix-quarter-and-fuel-source-gb

[2] T. Breithaupt, D. Herwig, L. Hofmann, *et al.*, "MIGRATE D1.1 Report on systemic issues." Dec. 15, 2016.

[3] A. Keane, L. Ochoa, C. Borges, *et al.*, "State-of-the-Art Techniques and Challenges Ahead for Distributed Generation Planning and Optimization," *IEEE Trans. Power Syst.*, vol. 28, no. 2, pp. 1493–1502, May 2013, doi: 10.1109/TPWRS.2012.2214406.

[4] R. Zuelli, R. Chiumeo, C. Gandolfi, *et al.*, "The impact of MVDC links on distribution networks," in *2018 AEIT International Annual Conference*, Bari, Italy, Oct. 2018, pp. 1–5. doi: 10.23919/AEIT.2018.8577442.

[5] A. Clerici, R. Chiumeo, and C. Gandolfi, "MVDC multi-terminal grids: a valid support for distribution grids improvement," in *2020 AEIT International Annual Conference (AEIT)*, Catania, Italy, Sep. 2020, pp. 1–6. doi: 10.23919/AEIT50178.2020.9241183.

[6] S. Hay, C. Cleary, G. McFadzean, *et. al*, "MVDC Technology Study - Market Opportunities and Economic Impact," TNEI Services Ltd, Manchester, UK, 9639-01-R0, Feb. 2015.

[7] J. Van Putten, J. Antolin Morales, V. Sewdien, *et al.*, "Capabilities and requirements definition for power electronics based technology for secure and efficient system operation and control," CIGRE, Paris, France, C2/B4, Nov. 2020.

[8] J. Morren, S. W. H. de Haan, W. L. Kling, *et al.*, "Wind Turbines Emulating Inertia and Supporting Primary Frequency Control," *IEEE Trans. Power Syst.*, vol. 21, no. 1, pp. 433–434, Feb. 2006, doi: 10.1109/TPWRS.2005.861956.

[9] M. Paolone, T. Gaunt, X. Guillaud, *et al.*, "Fundamentals of power systems modelling in the presence of converter-interfaced generation," *Electr. Power Syst. Res.*, vol. 189, p. 106811, Dec. 2020, doi: 10.1016/j.epsr.2020.106811.

[10] T. Ackermann, T. Prevost, V. Vittal, *et al.*, "Paving the Way: A Future Without Inertia Is Closer Than You Think," *IEEE Power Energy Mag.*, vol. 15, no. 6, pp. 61–69, Nov. 2017, doi: 10.1109/MPE.2017.2729138.

[11] H.-P. Beck and R. Hesse, "Virtual synchronous machine," in *2007 9th International Conference on Electrical Power Quality and Utilisation*, Barcelona, Spain, Oct. 2007, pp. 1–6. doi: 10.1109/EPQU.2007.4424220.

[12] Q.-C. Zhong and G. Weiss, "Synchronverters: Inverters That Mimic Synchronous Generators," *IEEE Trans. Ind. Electron.*, vol. 58, no. 4, pp. 1259–1267, Apr. 2011, doi: 10.1109/TIE.2010.2048839.

[13] A. J. Roscoe, M. Yu, A. Dyśko, *et al.*, "A VSM (Virtual Synchronous Machine) Convertor Control Model Suitable for RMS Studies for Resolving System Operator / Owner Challenges," p. 8.

[14] S. D'Arco and J. A. Suul, "Virtual synchronous machines; Classification of implementations and analysis of equivalence to droop controllers for microgrids," in *2013 IEEE Grenoble Conference*, Grenoble, France, Jun. 2013, pp. 1–7. doi: 10.1109/PTC.2013.6652456.

[15] A. Tayyebi, D. Gross, A. Anta, *et al.*, "Frequency Stability of Synchronous Machines and Grid-Forming Power Converters," *IEEE J. Emerg. Sel. Top. Power Electron.*, vol. 8, no. 2, pp. 1004–1018, Jun. 2020, doi: 10.1109/JESTPE.2020.2966524.

[16] R. Ofir, U. Markovic, P. Aristidou, *et al.*, "Droop vs. virtual inertia: Comparison from the perspective of converter operation mode," in *2018 IEEE International Energy Conference (ENERGYCON)*, Limassol, Jun. 2018, pp. 1–6. doi: 10.1109/ENERGYCON.2018.8398752.

[17] J. Liu, Y. Miura, and T. Ise, "Comparison of Dynamic Characteristics Between Virtual Synchronous Generator and Droop Control in Inverter-Based Distributed Generators," *IEEE Trans. Power Electron.*, vol. 31, no. 5, pp. 3600–3611, May 2016, doi: 10.1109/TPEL.2015.2465852.

[18] D. Pan, X. Wang, F. Liu, *et al.*, "Transient Stability of Voltage-Source Converters With Grid-Forming Control: A Design-Oriented Study," *IEEE J. Emerg. Sel. Top. Power Electron.*, vol. 8, no. 2, pp. 1019–1033, Jun. 2020, doi: 10.1109/JESTPE.2019.2946310.

[19] P. Kundur, *Power System Stability and Control*. New York, USA: McGraw-Hill Education, 1995.

[20] C. Henderson, D. Vozikis, D. Holiday, *et al.*, "Assessment of grid-connected wind turbines with inertia response considering internal dynamics," p. 26, 2020.

[21] N. Pogaku, M. Prodanovic, and T. C. Green, "Modeling, Analysis and Testing of Autonomous Operation of an Inverter-Based Microgrid," *IEEE Trans. Power Electron.*, vol. 22, no. 2, pp. 613–625, Mar. 2007, doi: 10.1109/TPEL.2006.890003.

[22] *IEEE Guide for Planning DC Links Terminating at AC Locations Having Low Short-Circuit Capacities*. 1997.